Correlation effects in La, Ce, and lanthanide ions

M. S. Safronova,[1,2] U. I. Safronova,[3] and Charles W. Clark[2]

[1]*Department of Physics and Astronomy, 217 Sharp Lab, University of Delaware, Newark, Delaware 19716, USA*

[2]*Joint Quantum Institute, National Institute of Standards and Technology and the University of Maryland, Gaithersburg, Maryland 20899, USA*

[3]*Physics Department, University of Nevada, Reno, Nevada 89557, USA*

We carry out a comprehensive study of higher-order correlation effects to the excitation energies of La, La$^+$, Ce, Ce$^+$, Ce^{2+}, and Ce^{3+}. The calculations are carried out using two hybrid approaches that combine configuration interaction with second-order perturbation theory and the linearized coupled-cluster all-order method. Use of two approaches allows us to isolate the effects of third- and higher-order corrections for various configurations. We also study the contribution of higher partial waves and investigate methods to extrapolate the effect of omitted partial waves. The effects of the higher partial waves for the monovalent configuration of La^{2+} and Ce^{3+} are compared with analogous effects in multivalent configurations of La, La$^+$, Ce, Ce$^+$, and Ce^{2+}. Tests of our extrapolation techniques are carried out for several Cd-like lanthanide ions. The results of the present studies are of particular interest to the development of high-precision methods for treatment of systems with partially filled nf shells that are of current experimental interest for a diverse set of applications.

PACS number(s): 31.15.ac, 31.15.ag, 31.15.aj

I. INTRODUCTION

While tremendous progress has been made recently in high-precision atomic calculations, accurate treatment of correlations in systems with open nf shells remains a challenge. Accurate properties of lanthanides, actinides, and their ions are of interest for many current applications including studies of fundamental interactions, atomic clock research, analysis of astrophysical data, plasma science, studies of quantum degenerate gases, and quantum information.

For example, a number of lanthanide ions have been recently suggested as candidates for the development of atomic clocks, search for the variation of fine-structure constant α, and quantum information [1,2]. Dysprosium has been used for study of weak interactions (parity violation) [3,4] and for search of the variation of the fine-structure constant [5,6]. Lanthanides have recently become of interest in ultracold atomic physics. In 2014, sub-Doppler laser cooling and magneto-optical trapping of holmium was demonstrated [7]. Both Bose-Einstein condensates and quantum-degenerate Fermi gases have been produced in isotopes of dysprosium [8]. Schemes have been identified for generating a synthetic magnetic field and spin-orbit coupling in highly magnetic lanthanide atoms such as dysprosium [9]. Employing these atoms offers several advantages for realizing strongly correlated states and exotic spinor phases [10]. Erbium has been a subject of recent experimental work [11–13] owing to its possible use in a variety of applications, including narrow linewidth laser cooling and spectroscopy, unique collision studies, and degenerate bosonic and fermionic gases with long-range magnetic dipole coupling. Quantum information studies use Yb$^+$ [14] states for the realization of the quantum bit. A recent proposal identified holmium for quantum information applications, due to its rich ground hyperfine manifold of 128 states [15].

Photoabsorption [16–19], electron scattering [20,21], and inelastic x-ray scattering [22] by lanthanides near the $3d$ and $4d$ electron edges are important tools for understanding magnetic materials. They reveal atomiclike $4f$ features that show effects of orbital collapse similar to those we study here. This subject has been of active interest since the 1970s, when conflicting ideas emerged regarding the role of single particle versus collective excitations in photoabsorption by the atomic $4d$ shell of lanthanides and neighboring elements [23]. It has also arisen again in the interpretation of recent experiments on multiple ionization of Xe by intense extreme ultraviolet radiation produced at free-electron laser facilities [24–28].

In a number of these applications, accurate atomic theory is indispensable to the design and interpretation of experiments, with direct experimental measurement of relevant parameters being impossible or infeasible. It is also necessary to be able to evaluate the uncertainty of theoretical predictions: this requires understanding of the accuracy of the method and the importance of physics beyond the Dirac-Hartree-Fock approximation.

Since complete treatment of all electron correlations is not possible even for relatively light systems, the correlation interactions are generally separated into core-core, core-valence, and valence-valence sectors. For example, La is considered to have three valence electrons in a $6s^25d$ ground-state configuration outside of a closed Xe-like core that contains 54 electrons. The treatment of lanthanides thus separates into two major problems: (1) inclusion of valence-valence correlations, and (2) inclusion of core-core and core-valence correlations. We use a hybrid approach that combines configuration interaction (CI) with a linearized coupled-cluster all-order method leading to natural separation of these correlation effects. In this method, the coupled-cluster approach is used to construct an effective Hamiltonian that contains dominant core and core-valence correlation corrections to all orders. After the construction of the effective Hamiltonian, the CI method is then used to treat valence-valence correlations. The importance of various correlations will depend upon the number of core shells and valence electrons. For example, the valence CI space for excitations of two valence electrons can be numerically saturated, i.e., addition of the other configurations to the

valence CI space will not improve accuracy further. Efficient construction of the relatively complete CI spaces for several electrons is a difficult problem explored in this work. Omission of important CI configurations may lead to major errors. However, the higher-order core-valence correlations are also particulary important for lanthanides, and we study these contributions in detail here.

We carry out extensive study of various correlation effects to the excitation energies of La, La$^+$, Ce, Ce$^+$, Ce^{2+}, and Ce^{3+}. Our calculations are carried out using two hybrid approaches that combine configuration interaction with second-order perturbation theory and a linearized coupled-cluster all-order method. This allows us to isolate the effects of third- and higher-order corrections for various configurations. The inclusion of the core-valence effects involves sums over the partial waves that are usually truncated at relatively low values of l such as $l = 5$. We find that the effects of higher partial waves are large for states with the $4f$ electrons. We developed methods to extrapolate the contribution of these higher partial waves. We have conducted additional studies of such higher partial wave contributions in several Cd-like lanthanide ions, where clear comparison with monovalent systems is possible. The implication of this work for the development of further methodologies is discussed in our conclusion. We conclude that at least perturbative valence triple excitations have to be included into the all-order construction of the effective Hamiltonian to further improve the accuracy.

II. REVIEW OF CURRENT KNOWLEDGE OF STRUCTURE OF La, Ce, AND THEIR IONS

One of the first analyses of lanthanum spectra that included 540 lines in La, 728 lines in La$^+$, and 10 lines in La^{2+} was presented by Russell and Meggers [29] in 1932. The analyses of all three spectra were supported by measurements of Zeeman effects, which were interpreted with the aid of Landé theory. The splitting factors, i.e., g values, showed marked departure from the theoretical values for many levels, but the "sum rule" was valid wherever it was tested [29].

Preliminary analysis of the first spark spectrum of Ce and Ce$^+$ was performed by Albertson and Harrison [30] which identified the $4f5d6s$ and $4f5d^2$ as the lowest configuration in Ce$^+$. Absorption spectra of cerium was recorded by Paul [31] where approximately 600 lines were observed. For wavelengths less than 320 nm, the intensity of the absorption lines falls off very rapidly and very few were observed. Reviews of atomic spectra of rare-earth elements presented by Meggers [32] raised a lot of questions in identification of cerium spectra, including determination of Ce^{2+} ground state.

The third spectrum of cerium (Ce III) was investigated by Russell *et al.* [33] in 1937. 33 triplet and singlet terms of Ce^{2+} had been recognized, accounting for 294 lines, including almost all of the wavelengths exceeding 200 nm. The electron configurations $4f5d$, $4f6p$, $5d^2$, $4f6s$, $4f6d$, and $5d6s$ have been almost completely identified. The last three configurations showed evidence of jj coupling.

New description and analysis of Ce^{2+} was given by Sugar [34] in 1963 including 1700 lines not previously reported. The ground level of this ion was established as the $^3H_4$ state of the $4f^2$ electronic configuration. 126 newly

discovered energy levels were given, together with revised values of previously known levels. The ionization limit, at 161 955 cm^{-l}, was derived from the three members of the $4fnd$ series [34].

The second spectrum of cerium (Ce II) was compiled by Corliss [35] in the wavelength region between 250 and 2400 nm. For the 11 000 lines in the list, about 7500 were classified [35] as transitions between 192 odd levels and 288 even levels. The odd levels arise from five configurations $4f5d^2$, $4f5d6s$, $4f6s^2$, $4f^26p$, and $4f^3$, and the even levels from seven configurations $4f^26s$, $4f^25d$, $4f5d6p$, $4f6s6p$, $5d^3$, $5d^26s$, and $5d6s^2$.

Low-lying levels of Ce were analyzed in 1963 by Martin [36], who showed that the ground level is $6s^25d4f$ $^1G_4$, rather than $6s^24f^2$. The latter incorrect identification of the ground configuration can still be found in reference literature today [37]. The cerium spectrum emitted by an electrodeless lamp was observed by Verges *et al.* [38] in the wavelength region from 0.82 to 2.42 μm. From the 2076 lines observed, about 1100 lines have been classified as transitions in the energy-level system of Ce$^+$ and 400 as lines of Ce^{2+}.

One of the first NIST compilations of the La, La$^+$, Ce, Ce$^+$, and Ce^{2+} energies was published by Martin *et al.* [39]. Energy-level data were given for 66 atoms and atomic ions of the 15 elements lanthanum ($Z = 57$) through lutetium ($Z = 71$). These data were critically compiled from published and unpublished material. Only experimentally determined energy levels were included.

A compilation for the neutral and singly ionized atoms of cerium and lanthanum was published in 2005 by Sansonetti and Martin [40]. The wavelengths, intensities, and spectrum assignments were given for each element and the data for the approximately 12 000 lines of all elements were collected into a single table and sorted by the wavelength [40].

Quinet and Biémont [41] calculated Landé g factors for experimentally determined energy levels of La^{2+}. Configuration interaction and relativistic effects had been included in the computations using the relativistic Hartree-Fock (HFR) technique combined with a least-squares fitting of the Hamiltonian eigenvalues to the observed energy levels [41]. In 2004, Biémont and Quinet [42] presented an overview of the recent developments concerning the spectroscopic properties of lanthanide atoms and ions with nuclear charge $Z = 57$–71. That review was focused on advances made during the previous 20 years in the analysis of the spectra, transition probabilities, radiative lifetimes, hyperfine structures, and isotope shifts.

The relativistic coupled-cluster method was applied by Eliav *et al.* [43] to evaluate the ionization potentials and excitation energies of La$^+$ and La^{2+}. Good agreement with available experimental data was obtained. Large relativistic effects were observed, affecting transition energies by up to 2.5 eV even for lanthanum [43].

Recently, Dzuba *et al.* [44] calculated the scalar static polarizabilities of lanthanides and actinides. Among different atoms, numerical results for the ground state of the scalar polarizabilities of Ce and La were listed. The configuration interaction technique was used [44].

A systematic study of La^{2+} properties including energies, transition rates, lifetimes, and multipole polarizabilities was carried out in [45] using the all-order coupled-cluster method.

III. MONOVALENT CALCULATIONS

A. All-order method

The calculations for monovalent Ce^{3+} were carried out using the relativistic all-order method discussed in detail in the review [46]. Briefly, the wave function of the valence electron v in the single-double (SD) approximation can be represented as an expansion that contains all possible single and double excitations of the lowest-order wave function:

$$|\Psi_v\rangle = \left[1 + \sum_{ma} \rho_{ma} a_m^\dagger a_a + \frac{1}{2} \sum_{mnab} \rho_{mnab} a_m^\dagger a_n^\dagger a_b a_a \right.$$
$$\left. + \sum_{m \neq v} \rho_{mv} a_m^\dagger a_v + \sum_{mna} \rho_{mnva} a_m^\dagger a_n^\dagger a_a a_v \right] |\Phi_v\rangle. \quad (1)$$

Φ_v is the lowest-order atomic state function, which is taken to be the *frozen-core* Dirac-Hartree-Fock (DHF) wave function of a state v:

$$|\Phi_v\rangle = a_v^\dagger |0_C\rangle,$$

where $|0_C\rangle$ represents the DHF wave function of the closed [Xe] core. In Eq. (1), $a_i^\dagger$ and a_i are creation and annihilation operators, respectively. We refer to ρ_{ma}, ρ_{mv} as single-core and valence-excitation coefficients and to ρ_{mnab} and ρ_{mnva} as double-core and valence-excitation coefficients, respectively. The following letters are used to distinguish core, excited, and valence states throughout the text:

$$
\begin{array}{ll}
a,b,c & \text{core states,} \\
m,n,r & \text{excited states,} \\
v,w & \text{valence states,} \\
i,j,k,l & \text{any state.}
\end{array}
$$

In the single-double partial triple (SDpT) all-order method, valence triple excitations described by the term

$$\frac{1}{6} \sum_{mnrab} \rho_{mnrvab} a_m^\dagger a_n^\dagger a_r^\dagger a_b a_a a_v |\Phi_v\rangle$$

are included perturbatively to ρ_{mv} and correlation energy equations as described in [46]. To derive the equations for the excitation coefficients, the wave function Ψ_v, given by Eq. (1), is substituted into the many-body Schrödinger equation

$$H|\Psi_v\rangle = E|\Psi_v\rangle, \quad (2)$$

where the Hamiltonian $H = H_0 + V_I$ is the relativistic *no-pair* Hamiltonian

$$H_0 = \sum_i \epsilon_i a_i^\dagger a_i,$$

$$V_I = \frac{1}{2} \sum_{ijkl} g_{ijkl} a_i^\dagger a_j^\dagger a_l a_k - \sum_{ij} U_{ij} a_i^\dagger a_j, \quad (3)$$

g_{ijkl} are Coulomb matrix elements, and U_{ij} is taken to be a frozen-core DHF potential. The equation for the correlation energy is given by

$$\delta E_v = \sum_{ra} \tilde{g}_{vavr} \rho_{ra} + \sum_{rab} g_{abvr} \tilde{\rho}_{rvab} + \sum_{rna} g_{vbrn} \tilde{\rho}_{rnvb}, \quad (4)$$

where $\tilde{g}_{ijkl} = g_{ijkl} - g_{ijlk}$ and $\tilde{\rho}_{ijkl} = \rho_{ijkl} - \rho_{ijlk}$. While the correlation energy calculated in the single-double (SD)

approximation contains fourth- and higher-order terms, it is known to omit the part of the third-order contribution which we calculate separately and refer to as $E_{\text{extra}}^{(3)}$. The energy calculated in the SDpT approximation is complete in third order.

B. Estimation of higher partial wave contribution: Monovalent case

All m, n, r sums in the all-order equations or perturbation theory terms imply the sums over all possible excited states. For example, the sum over r in Eq. (4) is over all excited states with with quantum numbers $n_r l_r j_r m_r$, $j_r = l_r \pm 1/2$, and is carried out using a finite basis set method with B-splines [46]. The sum over the magnetic quantum numbers m is performed analytically. While the sum over the principal quantum number n is made finite by the use of the finite basis set method, the sum over the partial waves l has to be truncated at relatively low value of l, typically $l_{\max} = 6$ for the all-order computations. The effects of the higher partial waves can be extrapolated in second order. The second-order calculation is very fast and can be done with large values of $l_{\max}$, such as $l_{\max} = 10$ or 11 with the remainder extrapolated. In Table I, we list second-order and the all-order results calculated with $l_{\max} = 5$, $l_{\max} = 6$, and their difference that gives the contribution of $l = 6$ partial waves. The all-order SD results include the $E_{\text{extra}}^{(3)}$ contribution. Final second-order values include contributions extrapolated to $l_{\max} = \infty$. We list the difference of $l_{\max} = \infty$ and 6 results in the column labeled "$l > 6$." We find that the contribution of the $l = 6$ partial wave is very close to the extrapolated contribution of partial waves with $l > 6$. This empirical result was previously observed for Ag-like and In-like highly charged ions [1], so this simple rule appears to be valid for a wide variety of monovalent systems with $4f$ electrons. Therefore, we use the all-order $l = 6$ contribution listed in the last column of the table as an estimate of the all-order extrapolated contribution. We note that the use of the second-order extrapolation would overestimate the actual $l > 6$ contribution since the second order overestimates the correlation correction for Ce^{3+} by about 50%.

C. Energies of Ce^{3+} and the phenomenon of $4f$ "orbital collapse"

Contributions to removal energies of Ce^{3+} and comparison of the results calculated in different approximations with experiment are given in Table II in cm^{-1}. These include lowest-order DF result, second and third-order contributions, SD and SDpT all-order values, and the $E_{\text{extra}}^{(3)}$ part of the third order not accounted for by the SD method. The total third-order, SD all-order, and SDpT all-order removal energies are listed in the next three columns and are calculated as follows: the third-order total values are the sum of the DF, second-, and third-order contributions; the SD total values are the sum of the DF, SD, and $E_{\text{extra}}^{(3)}$ contributions; and the SDpT total values are the sum of the DF and SDpT contributions. The differences between the removal energies obtained in different approximations and experimental values [47] are listed in the last four columns of Table II in cm^{-1}. The

TABLE I. Comparison of the second-order and all-order values calculated with different number of partial waves. Final second-order values include extrapolated contribution to $l = \infty$. Units: cm^{-1}.

Ion	State	Second-order values					All-order values		
		$l_{max} = 5$	$l_{max} = 6$	$l_{max} = \infty$	$l = 6$	$l > 6$	$l_{max} = 5$	$l_{max} = 6$	$l = 6$
La^{2+}	$4f_{5/2}$	−38 895	−40 198	−41 473	−1302	−1275	−26 722	−27 758	−1036
	$4f_{7/2}$	−38 165	−39 455	−40 717	−1290	−1262	−26 367	−27 399	−1032
	$5d_{3/2}$	−11 159	−11 485	−11 845	−326	−360	−8330	−8540	−210
	$5d_{5/2}$	−10 657	−10 973	−11 322	−316	−349	−8034	−8239	−205
	$6s_{1/2}$	−8425	−8491	−8575	−66	−84	−6070	−6096	−26
	$6p_{1/2}$	−5446	−5493	−5548	−47	−55	−4271	−4299	−28
	$6p_{3/2}$	−4948	−4992	−5043	−44	−51	−3883	−3910	−27
Ce^{3+}	$4f_{5/2}$	−43 887	−45 388	−46 880	−1501	−1492	−28 710	−29 859	−1149
	$4f_{7/2}$	−43 275	−44 769	−46 252	−1494	−1483	−28 386	−29 533	−1147
	$5d_{3/2}$	−12 759	−13 147	−13 575	−388	−428	−9539	−9795	−256
	$5d_{5/2}$	−12 229	−12 606	−13 023	−377	−417	−9248	−9497	−249
	$6s_{1/2}$	−10 040	−10 121	−10 223	−81	−102	−7088	−7126	−38
	$6p_{1/2}$	−7160	−7224	−7297	−64	−73	−5506	−5544	−38
	$6p_{3/2}$	−6541	−6600	−6668	−59	−68	−5056	−5096	−40

comparison with experiment indicates anomalously large correlation corrections and contributions of higher orders for $4f$ states. The discrepancies between the $4f$ second-order energies with experiment are larger than those values for other states by at least a factor of 4 and are over 8500 cm^{-1}. The total third-order contributions and third-order parts arising from triple excitations $E_{extra}^{(3)}$ are also larger for $4f$ states than for any other states. Comparison of the third-order, SD, and SDpT results indicates that triple excitations are particularly important for the accurate evaluation of the correlation correction for the $4f$ states. Such anomalously large correlation corrections for the $4f$ states are due to the "orbital collapse" discussed in the following.

The phenomenon of $4f$ "orbital collapse" was discussed by M. G. Mayer in 1941 [49]. She noted that, for atomic numbers around $Z = 57$, the Thomas-Fermi model of the atom produces an effective double-well radial potential for f electrons: a deep, but narrow, inner well near the nucleus; and a shallow, but broad, well of the form (in atomic units) $V(r) \rightarrow 6r^{-2} - Z_{eff}r^{-1}$ for large electron nucleus distances r, where Z_{eff} is the spectrum number, e.g., $Z_{eff} = 1$ for La, $Z_{eff} = 2$ for La$^+$, etc. The $4f$ wave-function collapse in DHF calculations was discussed in [50,51].

For Cs ($Z = 55$), the $4f$ electron is localized in the outer potential well, and so is a classic example of a Rydberg electron. The Cs $4f$ orbital is almost the same as the $4f$ orbital of H ($Z = 1$): the experimental value of the effective principal quantum number of Cs $4f$ is $n^* = 3.978$ versus $n = 4$ for H $4f$. As Z increases along the Cs $5p^6 4f$ isoelectronic sequence, the inner well grows deeper, and at some point the $4f$ orbital becomes localized within the atom, in the vicinity of the other N-shell orbitals $4s$, $4p$, and $4d$.

Figure 1 shows the evolution of large component of the DHF $4f_{5/2}$ orbital along the Cs $5p^6 4f$ isoelectronic sequence. The presence of two potential wells is vividly suggested by the $4f$ orbital of Ba$^+$ $5p^6 4f$, which has two local maxima. This was noticed by Connerade and Mansfield [52] in the context of a HF calculation of Ba$^+$ $5p^6 4f$, and by Johnson and Guet [53] in a many-body perturbation theory (MBPT) study of f-wave scattering of electrons in the first three members of the Xe $5p^6$ isoelectronic sequence: Xe, Cs$^+$, and Ba^{2+}. For the $5p^6 4f$ isoelectronic sequence, the progression of orbital collapse is quite regular, but the balance between inner and outer wells is generally sensitive to details. For example, Johnson and Guet [53] were unable to get a satisfactory account of the low-energy phase shift for f-wave scattering by Ba^{2+}, until they introduced a phenomenological potential to

TABLE II. Contributions to removal energies of Ce^{3+} and comparison of the results calculated in different approximations with experiment [47]. Units: cm^{-1}.

| State	Contributions					Totals					Differences with expt.			
	DF	$E^{(2)}$	$E^{(3)}$	E^{SD}	$E_{extra}^{(3)}$	E^{SDpT}	$E^{(2)}$	$E^{(3)}$	E^{SD}	E^{SDpT}	Expt.	$E^{(2)}$	$E^{(3)}$	E^{SD}	E^{SDpT}
$4f_{5/2}$	−262 168	−46 762	16 126	−38 021	7013	−32 470	−308 930	−292 804	−293 176	−294 638	−297 670	11 260	4866	4494	3032
$4f_{7/2}$	−260 351	−46 135	15 858	−37 581	6901	−32 100	−306 486	−290 628	−291 031	−292 451	−295 417	11 069	4789	4386	2966
$5d_{3/2}$	−236 832	−13 541	3886	−11 766	1715	−10 271	−250 373	−246 487	−246 883	−247 103	−247 933	2440	1446	1050	830
$5d_{5/2}$	−234 738	−12 991	3643	−11 354	1608	−9934	−247 729	−244 086	−244 484	−244 672	−245 444	2285	1358	960	772
$6s_{1/2}$	−203 193	−10 210	1027	−8743	1579	−7439	−213 403	−209 666	−210 357	−210 632	−211 068	2335	1402	711	436
$6p_{1/2}$	−168 882	−7287	2369	−6624	1042	−5742	−176 169	−173 800	−174 464	−174 624	−175 085	1084	1285	621	461
$6p_{3/2}$	−164 655	−6659	2155	−6079	945	−5282	−171 314	−169 159	−169 789	−169 937	−170 378	936	1219	589	441
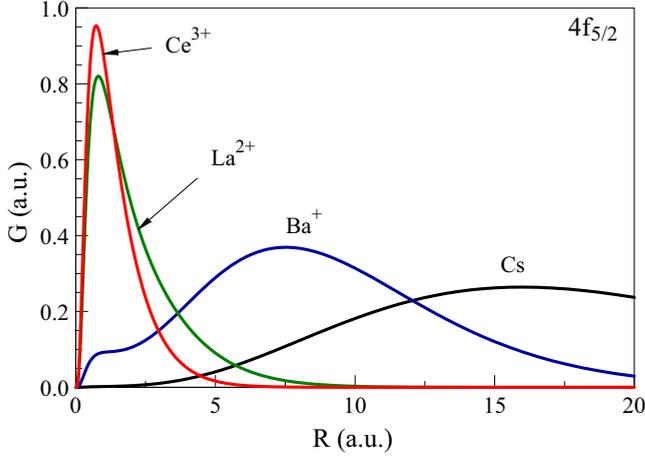
FIG. 1. (Color online) Large component of the $4f_{5/2}$ orbital in the $5s^25p^64f_{5/2}$ level of Cs, Ba$^+$, La^{2+}, and Ce^{3+} as calculated in the DHF approximation.

represent the effects of core polarization. No such potential was needed to get satisfactory agreement with experiment for the phase shifts for electron scattering by Xe or Cs$^+$, or for any other partial wave in electron scattering by Ba^{2+}. Evidently the core polarization potential is not particularly strong, but it is sufficient to tip the balance between inner and outer potential wells in Ba. Another such example is found [48] in Cs$^+4d^94f5s^25p^6$, which is an analog of Ce^{3+} due to the $4d$ hole. There, the Hartree-Fock $4f$ orbitals of different LS terms display the full range of behavior depicted in Fig. 1, as is shown in Fig. 2. In the $4d$ photoabsorption spectrum of the Ba isonuclear sequence, oscillator strength is shifted dramatically from the continuum into the discrete spectrum in the transition from Ba to Ba^{2+} [54,55]. Thus, orbital collapse amplifies the effects of correlation in $4f$ states in this region of the periodic table, and makes their accurate calculation particularly challenging compared to what is possible for states with no $4f$ occupancy.
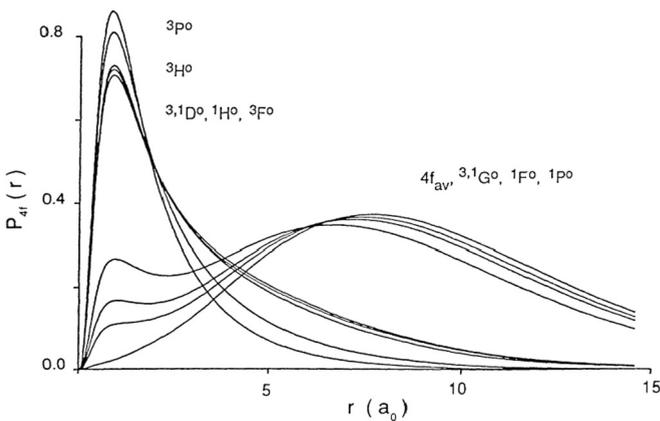

FIG. 2. The $4f$ orbitals of the ^1P, ^3P, ^1D, ^3D, ^1F, ^3F, ^1G, ^3G, ^1H, and ^3H terms of the configuration Cs$^+4d^94f5s^25p^6$, and of the "term-averaged" orbital as calculated in the term-dependent HF approximation. Labels, as read from top to bottom and left to right, are in order of increasing energy and radius of the orbital maximum. Reproduced from Ref. [48].

IV. CI + MBPT AND CI + ALL-ORDER METHODS

We carry out calculations for systems with two, three, and four valence electrons using both CI + MBPT and more accurate CI + all-order methods to establish the effect of the higher orders. The CI + MBPT method was developed in Ref. [56] and applied to the calculation of atomic properties of various systems in a number of previous works. In the CI method, the many-electron wave function is obtained as a linear combination of all distinct states of a given angular momentum J and parity:

$$\Psi_J = \sum_i c_i \Phi_i,$$

and energies and wave functions of the low-lying states are determined by diagonalizing the Hamiltonian:

$$H = H_1 + H_2.$$

The first part of the Hamiltonian H_1 represents the one-body part of the Hamiltonian, and H_2 represents the two-body part, which contains either Coulomb g_{ijkl} or Coulomb + Breit matrix elements. The precision of the CI method is drastically limited for large systems by the number of configurations that can be included. The CI + MBPT approach allows one to incorporate core excitations in the CI method by constructing an effective Hamiltonian that includes second-order terms: $H_1 \rightarrow H_1 + \Sigma_1$, and $H_2 \rightarrow H_2 + \Sigma_2$. The CI method is then applied as usual with the modified H^{eff} to obtain improved energies and wave functions

The second-order matrix elements $(\Sigma_1^{(2)})_{yx}$ are given by [57]

$$\left(\Sigma_1^{(2)}\right)_{yx} = \sum_{mab} \frac{g_{myab}\,\tilde{g}_{mxab}}{\epsilon_{ab} - \epsilon_{xm} + \tilde{\epsilon}_y - \epsilon_y} + \sum_{mna} \frac{g_{mnxa}\,\tilde{g}_{mnya}}{\tilde{\epsilon}_y + \epsilon_a - \epsilon_{mn}}.$$

(5)

In the equation above, the one-particle energies ϵ_i are written together as $\epsilon_{ij} = \epsilon_i + \epsilon_j$ for brevity. The summation over index i implies the sum over the quantum numbers $n_i\,\kappa_i\,m_i$. While the energy $\tilde{\epsilon}_y$ should be calculated from the particular eigenvalue of the effective Hamiltonian, we use the practical solution to set the energy $\tilde{\epsilon}_y$ to the Dirac-Fock energy of the lowest orbital for the particular partial wave.

The second-order matrix elements $(\Sigma_2^{(2)})_{mnvw}$ are given by [57]

$$\left(\Sigma_2^{(2)}\right)_{mnvw} = \sum_{cd} \frac{g_{vwcd}\,g_{mncd}}{\epsilon_{cd} - \epsilon_{mn} + \tilde{\epsilon}_v - \epsilon_v + \tilde{\epsilon}_w - \epsilon_w}$$

$$+ \left[\sum_{rc} \frac{\tilde{g}_{wrnc}\,\tilde{g}_{mrvc}}{\tilde{\epsilon}_v + \epsilon_c - \epsilon_{mr} + \tilde{\epsilon}_w - \epsilon_w} \right.$$

$$\left. + \begin{pmatrix} m & \Leftrightarrow & n \\ v & \Leftrightarrow & w \end{pmatrix}\right].$$

(6)

Since the expression above involves the sums over the excited states, the construction of the effective Hamiltonian also involves the truncation of the higher partial wave contribution described in Sec. III B. We discuss this issue in detail in Sec. IV A.

In the CI + all-order approach [57–61] corrections to the effective Hamiltonian are calculated using the variant of the

linearized single-double coupled cluster (all-order method) described in Sec. III A. To implement CI + all-order method, the all-order equations discussed in Sec. III A are rewritten in terms of the quantities Σ instead of the excitation coefficients ρ as follows:

$$\Sigma_{ma} = \rho_{ma}(\epsilon_a - \epsilon_m),$$
$$\Sigma_{mnab} = \rho_{mnab}(\epsilon_{ab} - \epsilon_{mn}), \qquad (7)$$
$$\Sigma_{mnva} = \rho_{mnva}(\tilde{\epsilon}_v + \epsilon_a - \epsilon_{mn}).$$

The quantities Σ_{ma}, Σ_{mnab}, and Σ_{mnva} are used in the all-order iteration procedure but do not explicitly appear in the effective Hamiltonian. The terms that contain no core summations are excluded from the equations to avoid double counting of such terms by the CI part of the calculations. The one-body correction to the effective Hamiltonian Σ_1 is given by

$$(\Sigma_1)_{mv} = \rho_{mv}(\tilde{\epsilon}_v - \epsilon_m), \qquad (8)$$

where ρ_{mv} are valence-excitation coefficients. The two-body correction to the effective Hamiltonian Σ_2 is constructed using the final Σ_{ma}, Σ_{mv}, Σ_{mnab}, and Σ_{mnva} values (see [57] for complete expressions). The CI method is then used to evaluate valence-valence correlations. Therefore, the effective Hamiltonian in the CI + all-order method contains dominant core and core-valence correlation corrections to all orders.

A. Estimation of higher partial wave contributions: Multivalent case

It is interesting to explore whether the partial wave contributions obtained for the states of monovalent systems such as Ce^{3+} are consistent with similar contributions that arise from the construction of Σ_1 and Σ_2 corrections to the effective Hamiltonian for the multivalent systems. To analyze this issue, we first study this effect in highly charged Cd-like ions that also have low-lying states with $4f$ electrons. Although these systems differ considerably from those that are the principal subjects of this paper, they exhibit the effects of

$4f$ correlation with great clarity, and in a way which sheds light on systematics observed in low-ionization stages. This selection of Cd-like ions is particularly interesting due to the change of the order of levels within this sequence of ions described in detail in [1].

The contribution of the $l = 6$ partial wave to the two-electron energies of Cd-like La^{9+}, Ce^{10+}, Pr^{11+}, Nd^{12+}, Sm^{14+} ions in cm^{-1} is given in Table III. These values are obtained as the differences of the CI + all-order calculations where effective Hamiltonian was constructed with $l_{max} = 6$ and with 5, respectively. We find that the divalent $l = 6$ values are nearly equal to the sum of the corresponding monovalent (Ag-like) $l = 6$ contributions [1,2], which are quite similar to the corresponding contribution for La^{2+} and Ce^{3+} listed in Table I. While there is a small increase in the value for ions with higher degree of ionization, each $4f$ electron contributes 1150–1300 cm^{-1} and each $5s$ or $5p$ electron contributes 150–200 cm^{-1}. These contributions from two electrons can simply be added to obtain the data for the Cd-like ions, with $4f^2$ state $l = 6$ contribution being about twice that of the states with only one $4f$ electron since $5s$ or $5p$ contributions are so small.

Next, we explore the partial wave truncation for Ce, La, and their ions. We begin by showing results for Ce in Table IV where we list the CI + all-order 4-electron energies (in cm^{-1}) of the lowest states of neutral cerium calculated with different numbers of partial waves. As in the previous example with Cd-like ions, these values are obtained by constructing the effective Hamiltonian with $l_{max} = 5$ and with $l_{max} = 6$, respectively. The column $l = 6$ gives the contribution of this partial wave, calculated as the difference of two previous columns. Similar monovalent and divalent cases were listed in Tables I and III, respectively. To compare the four-electron $l = 6$ values for Ce with one-electron $l = 6$ contributions for Ce^{3+}, we sum four respective one-electron $l = 6$ contributions $E_{l=6}$ for Ce^{3+} listed in the last column of Table I according to the electronic configuration. For example, the value for the $4f5d6s^2$ configuration was obtained as

TABLE III. Contribution of $l = 6$ partial wave to the two-electron energies of Cd-like ions in cm^{-1}.

Cd-like La^{9+}			Cd-like Ce^{10+}			Cd-like Pr^{11+}			Cd-like Nd^{12+}			Cd-like Sm^{14+}		
Level		$l = 6$	Level		$l = 6$	Level		$l = 6$	Level		$l = 6$	Level		$l = 6$
$5s^2$	$^1S_0$	−358	$5s^2$	$^1S_0$	−374	$5s^2$	$^1S_0$	−387	$5s^2$	$^1S_0$	−400	$4f^2$	$^3H_4$	−2760
$5p^2$	$^3P_0$	−353	$5p^2$	$^3P_0$	−387	$4f^2$	$^1G_4$	−2501	$4f^2$	$^3H_4$	−2600	$4f^2$	$^3H_5$	−2755
$5p^2$	$^3P_1$	−341	$4f5p$	$^3G_3$	−1407	$4f^2$	$^3H_5$	−2497	$4f^2$	$^3H_5$	−2596	$4f^2$	$^3F_2$	−2720
$5p^2$	$^1D_2$	−351	$4f5p$	$^3F_2$	−1374	$4f^2$	$^3H_6$	−2492	$4f^2$	$^3H_6$	−2591	$4f^2$	$^3H_6$	−2751
$5p^2$	$^3P_2$	−363	$4f5p$	$^3F_3$	−1402	$4f^2$	$^3F_2$	−2441	$4f^2$	$^3F_2$	−2562	$4f^2$	$^3F_3$	−2720
$4f5p$	$^3G_3$	−1326	$4f5p$	$^3G_4$	−1410	$4f^2$	$^3F_3$	−2439	$4f^2$	$^3F_3$	−2561	$4f^2$	$^1G_4$	−2723
$4f5p$	$^3F_3$	−1316	$4f^2$	$^1G_4$	−2439				$4f^2$	$^1G_4$	−2563	$4f^2$	$^3F_4$	−2717
$4f5p$	$^3F_2$	−1277	$4f^2$	$^3F_4$	−2454				$4f^2$	$^3F_4$	−2558	$5s^2$	$^1S_0$	−481
$5s5p$	$^3P_0$	−359	$5s5p$	$^3P_0$	−378	$4f5s$	$^3F_2$	−1474	$5s4f$	$^3F_2$	−1529	$4f5s$	$^3F_2$	−1619
$5s5p$	$^3P_1$	−356	$5s5p$	$^3P_1$	−375	$4f5s$	$^1F_3$	−1473	$5s4f$	$^3F_3$	−1528	$4f5s$	$^3F_3$	−1618
$5s5p$	$^3P_2$	−346	$4f5s$	$^3F_2$	−1412	$4f5s$	$^3F_4$	−1468	$5s4f$	$^3F_4$	−1523	$4f5s$	$^3F_4$	−1613
$5s5p$	$^1P_1$	−338	$4f5s$	$^3F_3$	−1410	$4f5s$	$^3F_3$	−1475	$5s4f$	$^1F_3$	−1529	$4f5s$	$^1F_3$	−1618
$4f5s$	$^3F_2$	−1334	$5s5p$	$^3P_2$	−364	$5s5p$	$^3P_0$	−392	$5s5p$	$^3P_1$	−405	$5s5p$	$^3P_0$	−435
$4f5s$	$^3F_3$	−1332	$4f5s$	$^3F_4$	−1405	$5s5p$	$^1P_1$	−390	$5s5p$	$^3P_2$	−392	$5s5p$	$^3P_1$	−432
$4f5s$	$^3F_4$	−1328	$4f5s$	$^1F_3$	−1414	$5s5p$	$^3P_2$	−378	$5s5p$	$^1P_1$	−384	$5s5p$	$^3P_2$	−418
$4f5s$	$^1F_3$	−1336	$5s5p$	$^1P_1$	−356	$5p5d$	$^1P_1$	−370				$5s5p$	$^1P_1$	−411

TABLE IV. The CI + all-order four-electron energies (in cm^{-1}) of the lowest states of neutral cerium calculated with different number of partial waves. The last column gives an estimate of $l = 6$ contribution in Ce based on the sum of four respective one-electron $l = 6$ contributions for Ce^{3+} from Table I.

Level		$l_{max} = 5$	$l_{max} = 6$	$l = 6$	One-el.
$4f5d6s^2$	$^1G_4$	−596 039	−597 526	−1487	−1476
$4f5d6s^2$	$^3F_2$	−596 061	−597 535	−1474	−1476
$4f5d6s^2$	$^3H_4$	−594 572	−596 065	−1493	−1476
$4f5d^26s$	$^5H_4$	−593 521	−595 088	−1567	−1690
$4f5d^26s$	$^5H_3$	−593 230	−594 767	−1536	−1690
$4f^26s^2$	$^3H_4$	−593 280	−595 623	−2343	−2372
$4f^26s^2$	$^3H_5$	−591 766	−594 104	−2337	−2372
$4f^26s^2$	$^3H_6$	−590 176	−592 506	−2330	−2372
$4f5d6s6p$	$^3F_2$	−581 265	−583 337	−2072	−1477
$4f5d6s6p$	$^3D_2$	−577 074	−579 134	−2060	−1477

$E_{l=6}(4f) + E_{l=6}(5d) + 2 \times E_{l=6}(6s) = -1148 \text{ cm}^{-1} - 252$ cm$^{-1} - 2 \times 38$ cm$^{-1} = -1476$ cm^{-1}, where we averaged $j = l \pm 1/2$ $E_{l=6}$ values. These results are listed in the last column of Table IV labeled "One-el." We find that these approximate one-electron values match the actual four-electron values very closely for the $4f5d6s^2$ and $4f^26s^2$ configurations. The results for other configurations are affected by configuration mixing, for example, $4f5d6s6p$ is strongly mixed with configurations containing two $4f$ electrons causing the actual $l = 6$ contribution to exceed the simple one-electron estimate. The $l = 6$ values for Ce$^+$, Ce^{2+}, La, and La$^+$ are essentially the same as for the neutral Ce example. Our results very clearly show that the multivalent case still follows the one-electron partial wave convergence pattern. Then, our empirical finding that the contributions from all partial waves with $l > 6$ should contribute about the same as $l = 6$ partial wave is also valid for the multivalent case.

V. RESULTS FOR Ce, La, AND THEIR IONS

Comparison of the CI + MBPT and CI + all-order energy levels (in cm^{-1}) with experiment [47] is given in Table V for La and La$^+$ and in Table VI for Ce, Ce$^+$, and Ce^{2+}. These tables give a representative sample of various configurations which most clearly illustrate the higher-order correlation correction in lanthanides.

A. La and La$^+$

We find excellent agreement of the La CI + all-order results with experiment with the exception of the $4f6s^2$ $^2F_{5/2}$ level. This is expected due to very large contributions of the higher orders for any configuration that involves the $4f$ state: note that the higher-order contribution is 4531 cm^{-1} for this level. As we show in the following, this is consistent with the difference of the Ce^{3+} energy levels with experiment given in Table II. In the case of La$^+$, all low-lying odd configurations contain one $4f$ electron, and the respective differences with experiment and higher-order contributions are very similar to those for the $4f6s^2$ $^2F_{5/2}$ level of La. Strong mixing of the $4f6s^2$ $^2F_{5/2}$ and $5d6s6p$ $^4F_{5/2}$ levels leads to slightly better agreement with

TABLE V. Comparison of the CI + MBPT and CI + all-order energy levels (in cm^{-1}) with experiment [47] for La and La$^+$. The higher-order contribution, estimated as the difference of the CI + all-order and CI + MBPT values, is listed in column "HO." The difference of the final all-order values with experiment is given in the last column.

	Level		J	MBPT	All	Expt.	HO	Diff.
La	$5d6s^2$	^2D	3/2	0	0	0	0	0
	$5d6s^2$	^2D	5/2	1136	1075	1053	−61	−22
	$5d^26s$	^4F	3/2	2538	2550	2668	12	118
	$5d^26s$	^4F	5/2	2917	2901	3010	−16	109
	$5d^26s$	^4F	7/2	3449	3395	3495	−54	100
	$5d^26s$	^4F	9/2	4146	4040	4122	−107	82
	$5d^26s$	^2F	5/2	7162	7025	7012	−137	−13
	$5d6s6p$	^4F	3/2	13 911	13 487	13 260	−424	−227
	$5d6s6p$		5/2	14 113	13 412	13 631	−700	219
	$5d6s6p$	^4D	1/2	14 773	14 326	14 096	−447	−230
	$5d6s6p$	^4D	3/2	15 261	14 871	14 709	−390	−162
	$5d6s6p$	^4F	5/2	15 817	15 382	14 804	−435	−578
	$5d6s6p$	^4F	7/2	15 528	14 814	15 020	−713	205
	$5d6s6p$		3/2	15 674	15 208	15 032	−466	−176
	$4f6s^2$	^2F	5/2	8719	13 250	15 197	4531	1947
	$5d6s6p$		1/2	15 845	15 407	15 220	−438	−187
	$5d6s6p$	^4D	5/2	16 038	15 660	15 504	−378	−156
La$^+$	$5d^2$	^3F	2	0	0	0	0	0
	$5d^2$	^3F	3	1093	1018	1016	−75	−2
	$5d^2$		2	1654	1543	1394	−110	−149
	$5d6s$	^3D	1	2188	2052	1895	−136	−157
	$5d^2$	^3F	4	2146	2002	1971	−144	−31
	$5d6s$	^3D	2	2956	2767	2592	−188	−176
	$5d6s$	^3D	3	3669	3439	3250	−230	−188
	$6s^2$	^1S	0	7753	7666	7395	−88	−271
	$4f6s$		2	6799	11 543	14 148	4744	2605
	$4f6s$		3	7000	11 740	14 375	4740	2635
	$4f6s$		4	8465	13 108	15 699	4643	2590
	$4f5d$	^1G	4	8840	13 237	16 599	4396	3362
	$4f5d$	^3F	2	9309	13 777	17 212	4468	3435
	$4f5d$	^3H	4	10 475	14 841	17 826	4366	2985

experiment for the $^2F_{5/2}$ La level than for the $4f6s$ levels of La$^+$ since configuration mixing reduces the "fraction" of the $4f$ electron in the $4f6s^2$ configuration in this case.

B. Ce, Ce$^+$, and Ce^{2+}

The higher-order contributions increase for Ce and its low-charged ions to 7500–8500 cm^{-1}. This leads to CI + MBPT giving the wrong ground state for Ce and Ce$^+$: all CI + MBPT results for even levels are *negative* indicating the wrong order with respect of the ground state. This is the most startling failure of the CI + MBPT method of which we are aware in systems with a few valence electrons. As a result, odd levels are shifted with respect to even levels, which is a well-known problem in lanthanides and actinides. The CI + all-order agreement with experiment is significantly improved, reducing even-odd shift by a factor of 3 to 4. The sources of the remaining odd-even shift are the missing triple and higher excitations in the construction of the effective Hamiltonian, as

TABLE VI. Comparison of the CI + MBPT and CI + all-order energy levels (in cm^{-1}) with experiment [47] for Ce, Ce$^+$, and Ce^{2+}. The higher-order contribution, estimated as the difference of the CI + all-order and CI + MBPT values, is listed in column "HO." The difference of the final all-order values with experiment is given in the last column.

	Level		J	MBPT	All	Expt.	HO	Diff.
Ce	$4f5d6s^2$	^{1}G	4	0	0	0	0	0
	$4f5d6s^2$	^{3}F	2	12	4	229	−8	225
	$4f5d6s^2$	^{3}H	4	1449	1455	1389	5	−66
	$4f5d^26s$	^{5}H	4	2428	2357	2438	−71	81
	$4f5d^26s$	^{5}H	3	2437	2710	2369	273	−341
	$4f^26s^2$	^{3}H	4	−6694	1047	4763	7741	3716
	$4f^26s^2$	^{3}H	5	−5017	2572	6239	7589	3667
	$4f^26s^2$	^{3}H	6	−3250	4177	7780	7427	3603
	$4f5d6s6p$	^{3}F	2	7736	13 604	14 646	5868	1042
	$4f5d6s6p$	^{3}D	2	12 306	17 818	16 534	5513	−1284
Ce$^+$	$4f5d^2$	^{4}H	7/2	0	0	0	0	0
	$4f5d^2$		9/2	1071	1062	988	−9	−75
	$4f5d^2$	^{4}I	9/2	1614	1771	1410	157	−361
	$4f5d^2$		1/2	2209	1897	2140	−312	243
	$4f5d6s$		5/2	2774	2838	2635	64	−203
	$4f^26s$	^{4}H	7/2	−7719	430	3854	8149	3424
	$4f^26s$	^{4}H	9/2	−7382	747	4166	8129	3419
	$4f^25d$	^{4}K	11/2	−3724	4053	7092	7776	3039
	$4f^26s$	^{4}F	3/2	−3391	4332	7455	7722	3123
	$4f^26s$	^{4}F	5/2	−3108	4603	7722	7712	3119
Ce^{2+}	$4f^2$	^{3}H	4	0	0	0	0	0
	$4f^2$	^{3}H	5	1704	1565	1528	−139	−37
	$4f^2$	^{3}H	6	3518	3227	3127	−291	−100
	$4f^2$	^{1}G	4	8526	7650	7120	−876	−530
	$4f^2$	^{1}D	2	15 122	13 786	12 835	−1336	−951
	$4f5d$	^{1}G	4	16 075	7529	3277	−8546	−4252
	$4f5d$	^{3}F	2	16 371	7865	3822	−8506	−4043
	$4f5d$	^{3}H	4	18 236	9614	5127	−8622	−4487
	$4f5d$	^{3}F	3	18 189	9862	5502	−8327	−4360
	$4f5d$	^{1}D	2	19 294	10 429	6571	−8864	−3858

is demonstrated by Table II that compares SD, SD+$E_{\text{extra}}^{(3)}$, and SDpT monovalent results. We do not observe deterioration of the agreement with experiment for Ce in comparison to Ce$^+$ and Ce^{2+}. This demonstrates that we included a sufficient number of configurations to effectively saturate the configuration space for this four-electron system.

Finally, we note that the contribution of the partial waves with $l > 5$ appears to have a sign that is opposite to that of the triple- and higher-excitation core-valence correlations that we presently omit at the construction of the effective Hamiltonian. The $l = 6$ partial wave contributes about 1200 cm^{-1} for any configuration involving a $4f$ electron, with $l > 6$ contributing another 1200 cm^{-1}, totaling 2400 cm^{-1} which is rather close

to the CI + all-order difference with respect to experiment. As a result, the $l_{\text{max}} = 5$ values agree very well with experiment, "conspiring to hide" the problem of higher-order contributions.

VI. CONCLUSION

We carried out extensive studies of various correlation effects on the excitation energies of La, La$^+$, Ce, Ce$^+$, Ce^{2+}, and Ce^{3+}, focusing specifically on the contribution of high partial waves and third- and higher-order corrections. Our calculations are carried out using two hybrid approaches that combine configuration interaction with second-order perturbation theory and a linearized coupled-cluster all-order method. This approach allows us to isolate the effects of third- and higher-order corrections for various configurations. Comparison of results for monovalent and multivalent systems allowed us to separately study the importance of the core-valence and valence-valence corrections. Our findings are summarized as follows:

(1) For the multivalent configurations, the correction due to high partial waves is largely determined by a number of $4f$ electrons in a configuration.

(2) The high partial wave contribution for multivalent systems mirrors the respective one-electron high partial wave contribution, unless significant mixing occurs between configurations with different numbers of the $4f$ electrons.

(3) For monovalent systems, we found empirically that the net correction for all partial waves with $l > 6$ was approximately equal to the contribution of a single $l = 6$ partial wave. Since the partial wave convergence for the multivalent case seems to follow the one-electron partial wave convergence pattern that empirical finding holds for multivalent systems.

(4) The third- and higher-order core-valence contribution is very large for configuration including the $4f$ electrons. This causes a large shift between odd and even configurations containing different numbers of $4f$ electrons.

(5) Strong cancellation is found between the $l > 5$ partial wave contributions and higher-order core-valence correlations.

In summary, the above problem of the even-odd configuration energy shift may be resolved by adding triple core-valence excitations to the construction of the effective Hamiltonian within the framework of the CI + all-order approach.

[1] M. S. Safronova, V. A. Dzuba, V. V. Flambaum, U. I. Safronova, S. G. Porsev, and M. G. Kozlov, Phys. Rev. Lett. **113**, 030801 (2014).

[2] M. S. Safronova, V. A. Dzuba, V. V. Flambaum, U. I. Safronova, S. G. Porsev, and M. G. Kozlov, Phys. Rev. A **90**, 042513 (2014).

[3] A. T. Nguyen, D. Budker, D. DeMille, and M. Zolotorev, Phys. Rev. A **56**, 3453 (1997).

[4] V. A. Dzuba and V. V. Flambaum, Phys. Rev. A **81**, 052515 (2010).

[5] S. J. Ferrell, A. Cingöz, A. Lapierre, A.-T. Nguyen, N. Leefer, D. Budker, V. V. Flambaum, S. K. Lamoreaux, and J. R. Torgerson, Phys. Rev. A **76**, 062104 (2007).

[6] A. Cingöz, A. Lapierre, A.-T. Nguyen, N. Leefer, D. Budker, S. K. Lamoreaux, and J. R. Torgerson, Phys. Rev. Lett. **98**, 040801 (2007).

[7] J. Miao, J. Hostetter, G. Stratis, and M. Saffman, Phys. Rev. A **89**, 041401 (2014).

[8] M. Lu, N. Q. Burdick, S. H. Youn, and B. L. Lev, Phys. Rev. Lett. **107**, 190401 (2011).

[9] X. Cui, B. Lian, T.-L. Ho, B. L. Lev, and H. Zhai, Phys. Rev. A **88**, 011601 (2013).

[10] M. Baranov, M. Dalmonte, G. Pupillo, and P. Zoller, Chem. Rev. **112**, 5012 (2012).

[11] A. Frisch, M. Mark, K. Aikawa, F. Ferlaino, J. L. Bohn, C. Makrides, A. Petrov, and S. Kotochigova, Nature (London) **507**, 475 (2014).

[12] K. Aikawa, A. Frisch, M. Mark, S. Baier, R. Grimm, and F. Ferlaino, Phys. Rev. Lett. **112**, 010404 (2014).

[13] A. Frisch, K. Aikawa, M. Mark, F. Ferlaino, E. Berseneva, and S. Kotochigova, Phys. Rev. A **88**, 032508 (2013).

[14] W. C. Campbell, J. Mizrahi, Q. Quraishi, C. Senko, D. Hayes, D. Hucul, D. N. Matsukevich, P. Maunz, and C. Monroe, Phys. Rev. Lett. **105**, 090502 (2010).

[15] M. Saffman and K. Mølmer, Phys. Rev. A **78**, 012336 (2008).

[16] A. Müller, S. Schippers, M. Habibi, D. Esteves, J. C. Wang, R. A. Phaneuf, A. L. D. Kilcoyne, A. Aguilar, and L. Dunsch, Phys. Rev. Lett. **101**, 133001 (2008).

[17] M. Habibi, D. A. Esteves, R. A. Phaneuf, A. L. D. Kilcoyne, A. Aguilar, and C. Cisneros, Phys. Rev. A **80**, 033407 (2009).

[18] A. Krisilov and B. Zon, Opt. Spectrosc. **109**, 833 (2010).

[19] G. Kutluk, H. Ishijima, M. Kanno, T. Nagata, and A. Domondon, J. Electron Spectros. **169**, 67 (2009).

[20] C. Dwyer, H. L. Xin, and D. A. Muller, Phys. Rev. B **86**, 094119 (2012).

[21] J. A. Bradley, K. T. Moore, G. van der Laan, J. P. Bradley, and R. A. Gordon, Phys. Rev. B **84**, 205105 (2011).

[22] G. van der Laan, Phys. Rev. B **86**, 035138 (2012).

[23] *Giant Resonances in Atoms, Molecules, and Solids*, edited by J. P. Connerade, J. M. Esteva, and R. C. Karnatak (Plenum, New York, 1987).

[24] A. A. Sorokin, S. V. Bobashev, T. Feigl, K. Tiedtke, H. Wabnitz, and M. Richter, Phys. Rev. Lett. **99**, 213002 (2007).

[25] M. Richter, M. Y. Amusia, S. V. Bobashev, T. Feigl, P. N. Juranić, M. Martins, A. A. Sorokin, and K. Tiedtke, Phys. Rev. Lett. **102**, 163002 (2009).

[26] M. Richter, J. Phys. B: At., Mol. Opt. Phys. **44**, 075601 (2011).

[27] P. Lambropoulos, K. G. Papamihail, and P. Decleva, J. Phys. B: At., Mol. Opt. Phys. **44**, 175402 (2011).

[28] A. S. Kornev, E. B. Tulenko, and B. A. Zon, Phys. Rev. A **84**, 053424 (2011).

[29] H. N. Russell and W. F. Meggers, Bur. Stand. J. Res. **9**, 625 (1932).

[30] W. E. Albertson and G. R. Harrison, Phys. Rev. **52**, 1209 (1937).

[31] F. W. Paul, Phys. Rev. **49**, 156 (1936).

[32] W. F. Meggers, Rev. Mod. Phys. **14**, 96 (1942).

[33] H. N. Russell, R. B. King, and R. J. Lang, Phys. Rev. **52**, 456 (1937).

[34] J. Sugar, J. Opt. Soc. Am. **53**, 831 (1963).

[35] C. H. Corliss, J. Res. Natl. Bur. Stand. (US) **77A**, 419 (1973).

[36] W. C. Martin, J. Opt. Soc. Am. **53**, 1047 (1963).

[37] Encyclopædia Britannica, online, http://www.britannica.com/EBchecked/topic/103535/cerium-Ce

[38] J. Verges, C. H. Corliss, and W. C. Martin, J. Res. Natl. Bur. Stand. (US) **76A**, 285 (1972).

[39] W. C. Martin, R. Zalubas, and L. Hagan, *Atomic Energy Levels-The Rare-Earth Elements* (National Bureau of Standards, Gaithersburg, MD, 1978).

[40] J. E. Sansonetti and W. C. Martin, J. Phys. Chem. Ref. Data **34**, 1559 (2005).

[41] P. Quinet and E. Biémont, At. Data Nucl. Data Tables **87**, 207 (2004).

[42] E. Biémont and P. Quinet, Phys. Scr. T **105**, 38 (2003).

[43] E. Eliav, S. Shmulyian, U. Kaldor, and Y. Ishikawa, J. Chem. Phys. **109**, 3954 (1998).

[44] V. A. Dzuba, A. Kozlov, and V. V. Flambaum, Phys. Rev. A **89**, 042507 (2014).

[45] U. I. Safronova and M. S. Safronova, Phys. Rev. A **89**, 052515 (2014).

[46] M. S. Safronova and W. R. Johnson, Adv. At. Mol. Opt. Phys. **55**, 191 (2007).

[47] Yu. Ralchenko, A. Kramida, J. Reader, and NIST ASD Team (2011). NIST Atomic Spectra Database (version 4.1). Available: http://physics.nist.gov/asd, National Institute of Standards and Technology, Gaithersburg, MD.

[48] C. W. Clark, Phys. Rev. A **35**, 4865 (1987).

[49] M. G. Mayer, Phys. Rev. **60**, 184 (1941).

[50] I. M. Band, V. I. Fomichev, and M. B. Trzhaskovskaya, J. Phys. B: At. Mol. Phys. **14**, 1103 (1981).

[51] I. M. Band and V. I. Fomichev, Phys. Lett. A **75**, 178 (1980).

[52] J. P. Connerade and M. W. D. Mansfield, Proc. R. Soc. London, Ser. A **346**, 565 (1975).

[53] W. R. Johnson and C. Guet, Phys. Rev. A **49**, 1041 (1994).

[54] T. B. Lucatorto, T. J. McIlrath, J. Sugar, and S. M. Younger, Phys. Rev. Lett. **47**, 1124 (1981).

[55] C. W. Clark, J. Opt. Soc. Am. B **1**, 626 (1984).

[56] V. A. Dzuba, V. V. Flambaum, and M. G. Kozlov, Phys. Rev. A **54**, 3948 (1996).

[57] M. S. Safronova, M. G. Kozlov, W. R. Johnson, and D. Jiang, Phys. Rev. A **80**, 012516 (2009).

[58] M. S. Safronova, M. G. Kozlov, and C. W. Clark, Phys. Rev. Lett. **107**, 143006 (2011).

[59] S. G. Porsev, M. S. Safronova, and M. G. Kozlov, Phys. Rev. A **85**, 062517 (2012).

[60] M. S. Safronova, S. G. Porsev, M. G. Kozlov, and C. W. Clark, Phys. Rev. A **85**, 052506 (2012).

[61] M. S. Safronova, S. G. Porsev, and C. W. Clark, Phys. Rev. Lett. **109**, 230802 (2012).